01 Jan 1977

Signal Processing for the Multistate Myoelectric Channel

Philip A. Parker

John A. Stuller
Missouri University of Science and Technology, stuller@mst.edu

R. N. Scott

Recommended Citation

P. A. Parker et al., "Signal Processing for the Multistate Myoelectric Channel," *Proceedings of the IEEE*, vol. 65, no. 5, pp. 662 - 674, Institute of Electrical and Electronics Engineers, Jan 1977.
The definitive version is available at https://doi.org/10.1109/PROC.1977.10545

[27] L. Lindström, R. Magnusson, and I. Petersén, "Muscle load influence on myo-electric signal characteristics," *Scand. J. Rehab. Med.*, suppl. 3, pp. 127-148, 1974.
[28] H. Broman, "An investigation on the influence of a sustained contraction on the succession of action potentials from a single motor unit," Res. Lab. Med. Electr., Göteborg, Sweden, Tech. Rep. 3:73, 1973.
[29] L. Lindström, "On cross-correlation measurements of myoelectric signals," Res. Lab. Med. Electr., Göteborg, Sweden, Tech. Rep. 11:74, 1974.
[30] S. Cobb and A. Forbes, "Electromyographic studies of muscular fatigue in man," *Am. J. Physiol.*, vol. 65, pp. 234-251, 1923.
[31] R. G. Edwards and O. C. J. Lippold, "The relation between force and integrated electrical activity in fatigued muscle," *J. Physiol.* (London), vol. 132, pp. 677-681, 1956.
[32] J. Scherrer and A. Bourguignon, "Changes in the electromyogram produced by fatigue in man," *Am. J. Physical Med.*, vol. 38, pp. 170-180, 1959.
[33] L. Lindström, R. Kadefors, and I. Petersén, "A new electromyographic index for muscle fatigue studies," in *Digest 11th Int. Conf. Medical and Biological Engineering* (Ottawa), 1976.
[34] ——, "An electromyographic index for localized muscle fatigue," manuscript submitted for publication.
[35] S. O. Rice, "Mathematical analysis of random noise," *Bell Syst. Tech. J.*, vol.'s 23, 24, pp. 1-162, 1944-1945.
[36] L. Lindström, H. Broman, R. Magnusson, and I. Petersén, "On the interrelation of two methods of EMG analysis," *Electroenceph. clin. Neurophysiol.*, vol. 34, p. 801, 1973.
[37] M. H. Dowling, P. Fitch, and R. G. Willison, "A special purpose digital computer (BIOMAC 500) used in the analysis of the human electromyogram," *Electroenceph. clin. Neurophysiol.*, vol. 25, pp. 570-573, 1968.
[38] A. Moosa and B. H. Brown, "Quantitative electromyography: A new analogue technique for detecting changes in action potential duration," *J. Neurol. Neurosurg. Psychiat.*, vol. 35, pp. 216-220, 1972.
[39] P. W. Nicholson, "Experimental models for current conduction in an anisotropic medium," *IEEE Trans. Biomed. Eng.*, vol. BME-14, p. 55, 1967.
[40] G. G. Macfarlane, "On the energy-spectrum of an almost periodic succession of pulses," *Proc. IRE*, vol. 37, pp. 1139-1143, 1949.
[41] H. P. Clamann, "Statistical analysis of motor unit firing patterns in a human skeletal muscle," *Biophys. J.*, vol. 9, pp. 1233-1251, 1969.
[42] H. S. Milner-Brown, R. B. Stein, and R. G. Lee, "Synchronization of human motor units: Possible roles of exercise and supraspinal reflexes," *Electroenceph. clin. Neurophysiol.*, vol. 38, pp. 245-254, 1975.
[43] R. S. Person and L. N. Mishin, "Auto- and cross-correlation analysis of the electrical activity of muscles," *Med. Electron. Biol. Engng.*, vol. 2, pp. 155-159, 1964.
[44] R. S. Person and M. S. Libkind, "Modelling of interference bioelectrical activity," *Biophysics (Biofizika)*, vol. 12, pp. 145-153, 1967.
[45] O. C. J. Lippold, J. W. T. Redfearn, and J. Vuco, "The electromyography of fatigue," *Ergonomics*, vol. 3, pp. 121-131, 1960.
[46] P. Rosenfalck, *Intra- and Extracellular Potential Fields of Active Nerve and Muscle Fibres.* Köbenhavn, Denmark: Akademisk Forlag, 1969.
[47] R. E. Pattle, "The external action potential of a nerve or muscle fibre in an extended medium," *Phys. Med. Biol.*, vol. 16, pp. 673-685, 1971.
[48] J. Ekstedt and E. Stålberg, "How the size of the needle electrode leading-off surface influences the shape of the single muscle fibre action potential in electromyography," *Computer Programs in Biomedicine*, vol. 3, pp. 204-212, 1973.
[49] R. Plonsey, "Volume conductor fields of action currents," *Biophys. J.*, vol. 4, pp. 317-327, 1964.
[50] J. Clark and R. Plonsey, "A mathematical evaluation of the core conductor model," *Biophys. J.*, vol. 6, pp. 95-112, 1966.

Signal Processing for the Multistate Myoelectric Channel

PHILIP A. PARKER, JOHN A. STULLER, AND R. N. SCOTT, SENIOR MEMBER, IEEE

Abstract—**In the multistate myoelectric channel, a single myoelectric signal source is used to control a multifunction powered prosthesis. The selection of a prosthesis function requires a receiver to process the myoelectric signal, contaminated with noise, and to decide on the basis of the received signal which function is desired. Thus the channel clearly presents a problem of choice of receiver and of decision strategy. Previous solutions to this problem have been basically empirical. In this paper we seek the optimum receiver where optimum is in the minimum probability of error sense. First a model is developed for the bipolar myoelectric signal to provide information about the relevant signal parameters and statistics. Using this information the Bayes minimum probability of error receiver is derived for an arbitrary signal parameter set. The optimum signal parameter set is then found for the Bayes receiver, and the receiver performance calculated. The receiver performance is measured and compared with the calculated performance. A significant performance improvement is seen in the optimum receiver over a more conventional receiver.**

Manuscript received May 13, 1976; revised August 27, 1976. This work was supported in part by the Canadian National Research Council and the Department of National Health and Welfare.

The authors are with the Bioengineering Institute and Electrical Engineering Department, University of New Brunswick, Fredericton, N.B., Canada.

I. INTRODUCTION

THE MYOELECTRIC channel has attracted considerable interest in the field of aids for the disabled, the most well known application being the control of powered prostheses [1], [2]. This paper deals with myoelectric signal processing for the multistate myoelectric channel.

The approach taken here is to view the human operator as a complex data gathering and processing system having various input–output information channels with which to communicate with his environment. His myoelectric channel is one in which information is conveyed to the machine via the electrical signal generated by an active skeletal muscle. A specific muscle is chosen as the signal source and a specific parameter γ of this signal is chosen as the information parameter. For the multistate myoelectric channel a set $\{\gamma_i: i = 0, 1, \cdots, M-1\}$, of discrete parameter values or states is used to designate the prosthesis functions where there are M possible functions. Each function is assigned a parameter value or state which the operator produces by generating the appropriate myoelectric signal. This process, contaminated by noise, is

then observed by the prosthesis receiver whose task it is to determine which function the operator intended. There are two engineering problems to be solved in this formulation. The first is the task of determining an "optimum" set of parameter values to be used, while the second is that of determining the "optimum" signal processing strategy. In Section II we discuss myoelectric signal processing in general. In Section III we develop a practically useful model of the myoelectric process for the bipolar electrode configuration. We then apply this model in Sections IV and V to obtain answers to the two questions posed.

II. Myoelectric Signal Processing

The signal processing strategy used in a myoelectric channel depends on the task to be performed by the channel and the performance criterion. Since these vary widely it is often impossible to compare directly the results found in the literature. However, this section is intended to place the work of this paper in perspective relative to that of other authors.

Signal processing problems in general can be classified as being either (i) estimation or (ii) detection problems. Estimation arises when dealing with a signal parameter which takes unknown values in a continuum of values over a given range. Here the object is to estimate the unknown value. This estimate is subject to error due to either or both additive noise and the statistical nature of the signal. The error standard deviation or the normalized error standard deviation (normalized to the mean of the estimate) is used as the estimation performance measure. Proportional myoelectric control of the elbow angle of a powered prosthesis is an example of the application of estimation. In this instance the angle is continuously related to some signal parameter. Hence an estimation of the parameter is required to specify the elbow angle over a given range.

The detection problem arises when dealing with a signal parameter which takes only values from a finite set of known values. The object is to decide, given the received signal, which of the possible known values the parameter currently takes. A receiver is required which processes the signal in some prescribed manner and compares the processor output with some predetermined decision boundaries. Since the result is either a correct or incorrect decision the appropriate performance measure is the probability of a correct decision. This is a significant difference from the estimation problem. The estimation problem performance measure, error standard deviation, is not sufficient for the detection problem: two receivers with the same error standard deviation can differ in their probabilities of a correct decision.

In this paper we place the multistate myoelectric channel problem in the framework of decision theory and formulate it as a detection problem. The intent is to find the signal processor and decision regions which will give the operator a minimum error probability in function selection where both the number of functions and the processing time are independent variables. To the knowledge of the authors this has not been attempted previously although there are related works. Kreifeldt [3] considers signal processing for the myoelectric channel. However, he is concerned with the estimation problem in application to proportional control. He uses the reciprocal of the normalized standard deviation, referred to as the signal-to-noise ratio (SNR), as the performance measure. Graupe *et al.*, [4] develop a time-series model for the myoelectric signal for application with a multifunction prosthesis. It involves a pattern recognition scheme and hence decision and detection theory are applicable. It differs significantly from the present work in that the approach utilizes several myoelectric signal sources. No attempt is made to determine the decision-making performance of the system.

III. Bipolar Myoelectric Signal Model

In this section we develop a model for the generation of the myoelectric signal obtained from the bipolar electrode configuration. The main results are summarized in items 1 to 6 at the end of the section.

A bipolar signal may be defined [5] as the potential difference between two electrodes both of which are placed in an active muscle region. This is as opposed to a monopolar signal which is the potential difference between an active and an inactive muscle region. The bipolar signal is of particular interest since it, rather than the monopolar signal, normally is used in the myoelectric channel. For the purpose of this model the depolarization-repolarization of a skeletal muscle fiber membrane constitutes the basic electrical event. The depolarization wavefront propagates the length of the fiber at a velocity of v meters per second, producing at any given point along the fiber a time varying potential field. Since all fibers of a motor unit are innervated by a common nerve axon, one can view the motor unit as a composite fiber. The motor unit's "action potential" at the given point near the unit, with respect to some remote reference, is the spatial sum of the time varying fields from the propagating depolarization wavefronts of all the unit's fibers with appropriate attenuation for the electrode location. The motor unit action potential is the basic signal element for the model. This signal element is, with each nerve axon innervation pulse, a repeatable function of time $p(t)$. The form of the action potential $p(t)$ depends on the velocity v and the position of the observation point relative to the fibers. It is not the intention of this paper to express $p(t)$ in terms of these variables. It is sufficient here to simply denote the observed action potential for the jth motor unit as $p_j(t)$. Thus the observed monopolar action potential pulse train, say $U_j(t)$, at the observation point for the jth unit is

$$U_j(t) = \sum_{i=1}^{\infty} a_j p_j(t - t_{ij}) \tag{1}$$

where a_j and t_{ij} are respectively the amplitude and the ith pulse time displacement for the jth motor unit. $U_j(t)$ can be considered [6] as the convolution of $a_j p_j(u)$ with a unit intensity impulse train, i.e.,

$$U_j(t) = \int_{-\infty}^{\infty} a_j p_j(t - u) \sum_{i=1}^{\infty} \delta(u - t_{ij})\, du$$

$$= a_j p_j(t) * Q_j(t)$$

where $\delta(u)$ is the Dirac delta function, $*$ denotes the convolution operation and

$$Q_j(t) = \sum_{i=1}^{\infty} \delta(t - t_{ij}).$$

Consider now a steady-state isometric contraction. The isometric restriction is, for the amputee, a reasonable one for the following reason. With all candidates for a multistate myoelectric control system a prime consideration in control site selec-

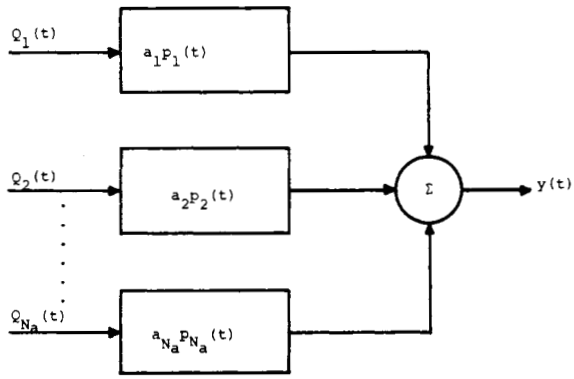

Fig. 1. Generation of $y(t)$ with different action potentials $p_j(t)$, $j = 1, 2, \cdots, N_a$.

tion is to find residual muscle just proximal to the amputation level which no longer acts across a joint and hence serves no normal function.[1] This leaves it free to be used as a control signal source. The distal end of such residual muscle is usually tied down or constrained by scar tissue. The muscle is thus essentially fixed at both ends, and contractions are at least approximately isometric.

If there are N_a active motor units in the steady-state muscle contraction the resultant monopolar myoelectric signal $y(t)$ is given by

$$y(t) = \sum_{j=1}^{N_a} U_j(t)$$

$$= \sum_{j=1}^{N_a} a_j p_j(t) * Q_j(t) \tag{2}$$

The following assumptions are now made:

1) $\int_{-\infty}^{\infty} p_j(u)\, du = 0$ for all $j, j = 1, 2, \cdots, N_a$;
2) the $Q_j(u)$, $j = 1, 2, \cdots, N_a$, are uncorrelated random point processes whose statistics differ only in their respective mean firing rates $\lambda_j, j = 1, 2, \cdots, N_a$.

The first assumption holds in practice due to the ac coupled signal amplifiers. The second assumption has been substantially justified by Clamman [7] and Shwedyk [8]. A block diagram realization of $y(t)$ according to (2) is shown in Fig. 1. It is easily seen that the autocovariance function $\phi_{yy}(\tau)$ of $y(t)$ is

$$\phi_{yy}(\tau) = \sum_{j=1}^{N_a} \phi_j(\tau)$$

where $\phi_j(\tau)$ is the autocovariance function of $U_j(t)$. The form of $\phi_j(\tau)$ depends on the form of $p_j(t)$. Since N_a is normally large it is expedient to obtain a simplified expression for $\phi_{yy}(\tau)$ by defining an average action potential $p(t)$ as [9]

$$p(t) = \begin{cases} t(2 - c_0 t) \exp(-c_0 t), & t \geq 0 \\ 0, & t < 0 \end{cases} \tag{3}$$

[1] A muscle which is still serving its normal functional role cannot also serve as a control signal site. It *may* be possible to retrain a normally functioning muscle to give up its normal function and serve as a control site. However, to the authors' knowledge, this difficult alternative has yet to be used clinically.

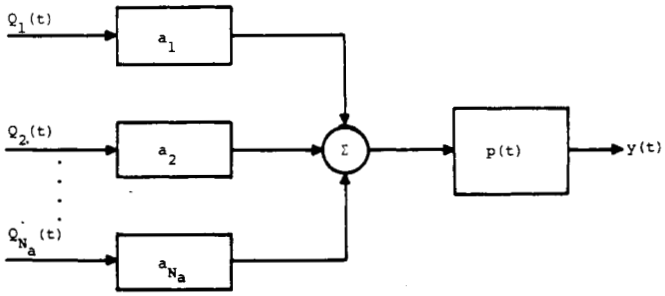

Fig. 2. Generation of $y(t)$ with an average action potential $p(t)$.

where c_0 is a constant. With this definition $y(t)$ becomes

$$y(t) = p(t) * \sum_{j=1}^{N_a} a_j Q_j(t) \tag{4}$$

This average action potential is based on observations of numerous motor unit action potentials from various skeletal muscles including the biceps brachii muscle.[2]

A block diagram realization of $y(t)$ according to (4) is shown in Fig. 2. Note that $p(u)$ is convolved with the sum of N_a impulse trains. The resultant of this sum can be considered a single composite point process

$$Q(t) = \sum_{j=1}^{N_a} \sum_{i=1}^{\infty} a_j \delta(t - t_{ij}).$$

To an observer, sample functions from $Q(t)$ would appear as impulse trains with random impulse intensities. Thus from a practical point of view one can represent $Q(t)$ as

$$Q(t) \simeq \sum_{k=1}^{\infty} a_k \delta(t - t_k)$$

where the a_k are uncorrelated random variables, each with mean μ_a and mean-square value ψ_a, and $t_{ij} \to t_k$. The monopolar signal $y(t)$ then becomes

$$y(t) \simeq \int_{-\infty}^{\infty} p(t - u) \sum_{k=1}^{\infty} a_k \delta(u - t_k)\, du$$

$$= p(t) * Q(t) \tag{5}$$

Consider now the bipolar electrode configuration in which two electrodes are spaced a distance d along the muscle fibers with both on the same side of the innervation zone. If $y(t)$ is the monopolar signal at one electrode and $z(t)$ the monopolar signal at the other, then the bipolar signal $s(t)$ is their difference, i.e.,

$$s(t) = y(t) - z(t) \tag{6}$$

Because of the action potential propagation it is obvious that $z(t)$ will be a sum of the action potentials which contribute to $y(t)$, delayed by an amount $\Delta = d/v$, i.e.,

$$z(t) = \sum_{j=1}^{N_a} b_j q_j(t) * Q_j(t - \Delta)$$

[2] There is no attempt to differentiate between "slow" and "fast" units since nothing in the literature suggests any difference as far as the action potential is concerned.

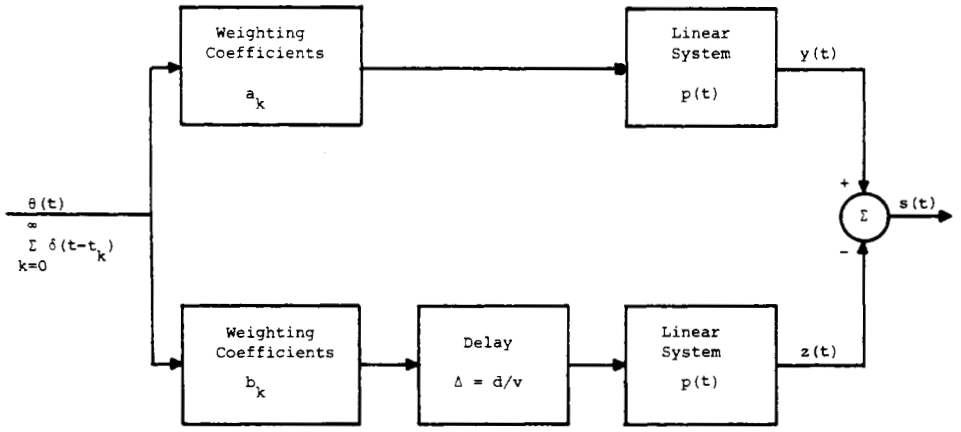

Fig. 3. Generation of bipolar signal $s(t)$.

where b_j and $q_j(t)$ are the scale factor and action potential pulse form respectively for the jth motor unit at the electrode associated with $z(t)$. Applying the same arguments to $z(t)$ about average waveform shape and composite point process, as to $y(t)$, gives

$$z(t) \simeq \int_{-\infty}^{\infty} p(t-u) \sum_{k=1}^{\infty} b_k \delta(u - t_k - \Delta)\, du$$

$$= p(t) * P(t) \tag{7}$$

where

$$P(t) = \sum_{k=1}^{\infty} b_k \delta(t - t_k - \Delta)$$

and the b_k are uncorrelated random variables each with mean μ_b and mean-square value ψ_b. Using (5)–(7) a block diagram realization of $s(t)$ is given in Fig. 3.

For large N_a and time intervals small compared to the individual motor unit average interspike interval, $Q(t)$ and $P(t)$ will both closely approximate Poisson point processes [10] each with the mean firing rate λ_p given by

$$\lambda_p = \sum_{j=1}^{N_a} \lambda_j.$$

Now the autocovariance function $\phi_{yy}(\tau)$, $\phi_{zz}(\tau)$, and $\phi_{ss}(\tau)$ for $y(t)$, $z(t)$ and $s(t)$, respectively, and the cross-covariance function $\phi_{yz}(\tau)$ are most easily determined by first obtaining the autocorrelation functions $R_{QQ}(\tau)$ and $R_{PP}(\tau)$ for the Poisson point process $Q(t)$ and $P(t)$, respectively, and the cross-correlation function $R_{QP}(\tau)$. For stationary Poisson point processes with random impulse intensities it is shown in Appendix I that

$$R_{QQ}(\tau) = \psi_a \lambda_p \delta(\tau) + \mu_a^2 \lambda_p^2, \tag{8}$$

$$R_{PP}(\tau) = \psi_b \lambda_p \delta(\tau) + \mu_b^2 \lambda_p^2 \tag{9}$$

$$R_{QP}(\tau) = \psi_{ab} \lambda_p \delta(\tau - \Delta) + \mu_a \mu_b \lambda_p^2. \tag{10}$$

Since $y(t)$ and $z(t)$ are the outputs of linear systems whose inputs are $Q(t)$ and $P(t)$ then (8)–(10) give [11]

$$\phi_{yy}(\tau) = \psi_a \lambda_p \int_{-\infty}^{\infty} p(u)\, p(u+\tau)\, du \tag{11}$$

$$\phi_{zz}(\tau) = \psi_b \lambda_p \int_{-\infty}^{\infty} p(u)\, p(u+\tau)\, du \tag{12}$$

and

$$\phi_{yz}(\tau) = \psi_{ab} \lambda_p \int_{-\infty}^{\infty} p(u)\, p(u+\tau-\Delta)\, du. \tag{13}$$

Let

$$\phi(\tau) = \int_{-\infty}^{\infty} p(u)\, p(u+\tau)\, du$$

and substituting (3) for $p(u)$ gives

$$\phi(\tau) = \left[\frac{1}{c_0^3} + \frac{|\tau|}{c_0^2} - \frac{\tau^2}{c_0}\right] \exp\left[-c_0|\tau|\right]. \tag{14}$$

Equations (11)–(13) then become

$$\phi_{yy}(\tau) = \psi_a \lambda_p \phi(\tau), \tag{15}$$

$$\phi_{zz}(\tau) = \psi_b \lambda_p \phi(\tau) \tag{16}$$

$$\phi_{yz}(\tau) = \psi_{ab} \lambda_p \phi(\tau - \Delta). \tag{17}$$

The autocovariance function $\phi_{ss}(\tau)$ for the bipolar signal $s(t)$ easily follows from (6), (15)–(17) and is given by

$$\phi_{ss}(\tau) = [\psi_a + \psi_b]\, \lambda_p \phi(\tau) - \psi_{ab} \lambda_p [\phi(\tau + \Delta) + \phi(\tau - \Delta)]. \tag{18}$$

The power density spectrum for $s(t)$, $\Phi_{ss}(\omega)$, is

$$\Phi_{ss}(\omega) = (\psi_a + \psi_b)\, \lambda_p \Phi(\omega)[1 - D \cos \omega\Delta] \tag{19}$$

where $\Phi(\omega)$ is the Fourier transform of $\phi(\tau)$ and $D = 2\psi_{ab}/(\psi_a + \psi_b)$. The dependence of the bipolar signal statistics on electrode spacing is obvious from (18) and (19). The effect can be seen by considering the statistical equivalent bandwidth B_s, [12], of $s(t)$ as a function of Δ where

$$B_s = \frac{\left[\int_0^{\infty} \Phi_{ss}(\omega)\, d\omega\right]^2}{2\pi \int_0^{\infty} \Phi_{ss}^2(\omega)\, d\omega} \text{ Hz} \tag{20}$$

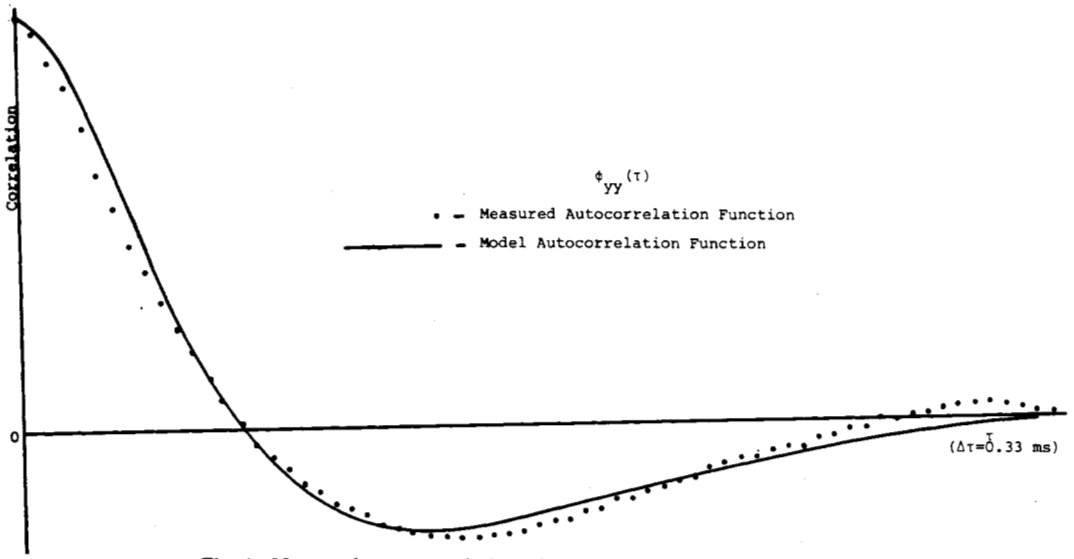

Fig. 4. Measured autocorrelation function, monopolar signal, compared with model (model coefficient $c_0 = 340$).

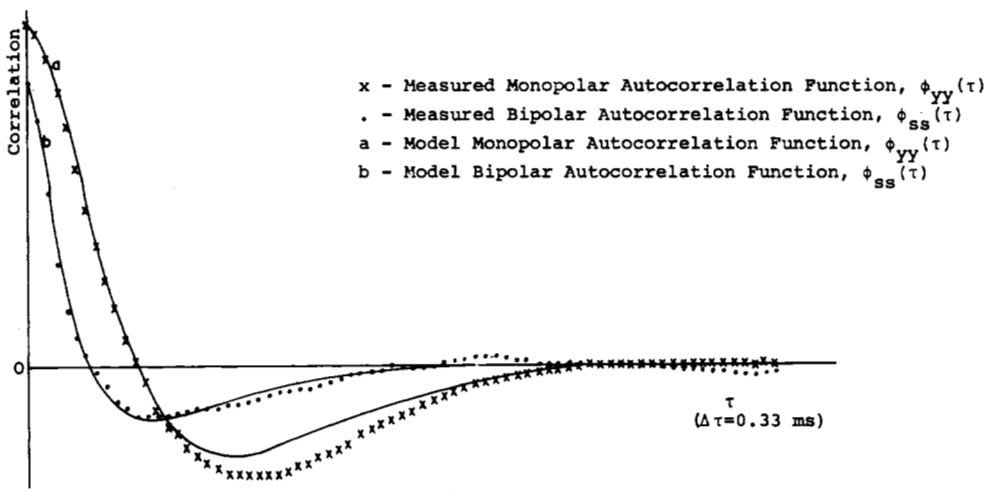

Fig. 5. Measured autocorrelation functions, monopolar and bipolar signals, compared with models (model coefficient $c_0 = 420$).

Putting (19) in (20) and carrying out the indicated operations gives

$$B_s = F_n/F_d \tag{21}$$

where

$$F_n = [1/c_0^2 - De^{-c_0\Delta}(1/c_0^2 + \Delta/c_0 - \Delta^2)]^2$$

$$F_d = 3(D^2+2)/2c_0^5 + (De^{-c_0\Delta}/30)[45(De^{-c_0\Delta} - 4)/c_0^5 + 45\Delta(2De^{-c_0\Delta} - 4)/c_0^4 - 15\Delta^3(8De^{-c_0\Delta} - 4)/c_0^2 - 5\Delta^4(10De^{-c_0\Delta} - 4)/c_0 + \Delta^5(32De^{-c_0\Delta} - 4)].$$

Two cases are of particular interest. For $\Delta = 0$, equation (21) gives

$$B_s = c_0/3 \text{ Hz}$$

which is the value of B_s for the monopolar signal as seen by evaluating (20) with $\Phi(\omega)$ replacing $\Phi_{ss}(\omega)$. For $\Delta = \infty$, equation (21) gives

$$B_s = \frac{2c_0}{3(D^2+2)}$$

which indicates that, for large Δ, B_s approaches a constant value which depends on D. Since $0 \leqslant D \leqslant 1$ the value of B_s, for $\Delta = \infty$, will be less than or equal to the monopolar signal bandwidth. From Fig. 7 it is seen that there is a value of Δ for which B_s is maximum. This is significant since to minimize signal parameter estimation error one wishes to maximize the signal bandwidth [12].

To verify these results, estimates of $\phi_{yy}(\tau)$, $\phi_{yz}(\tau)$, $\phi_{ss}(\tau)$, and B_s were found for monopolar and bipolar signals obtained from fine wire intramuscular electrodes in the proximal third of the long head of the biceps brachii muscle. The proximal third was used in order to avoid the innervation zone which lies in the distal third of this muscle [13]. Correlation functions were computed digitally with a minimum signal sample duration of 10 s and a maximum lag value of 33 ms. Equation (20) was evaluated numerically for estimates of B_s. Figs. 4 and 5 show the measured and theoretical autocorrelation functions $\phi_{yy}(\tau)$ and $\phi_{ss}(\tau)$ with $d = 0.5$ cm. The theoretical curves were obtained from (15) and (18) with the parameters c_0, $\lambda_p\psi_a$, $\lambda_p\psi_b$, and $\lambda_p\psi_{ab}$ obtained from the measured data. Fig. 6 shows estimates of $\phi_{yz}(\tau)$ for $d = 0.5$ and 1.0 cm and an estimate of $\phi_{yy}(\tau)$. The delay Δ is clearly seen. These values of d

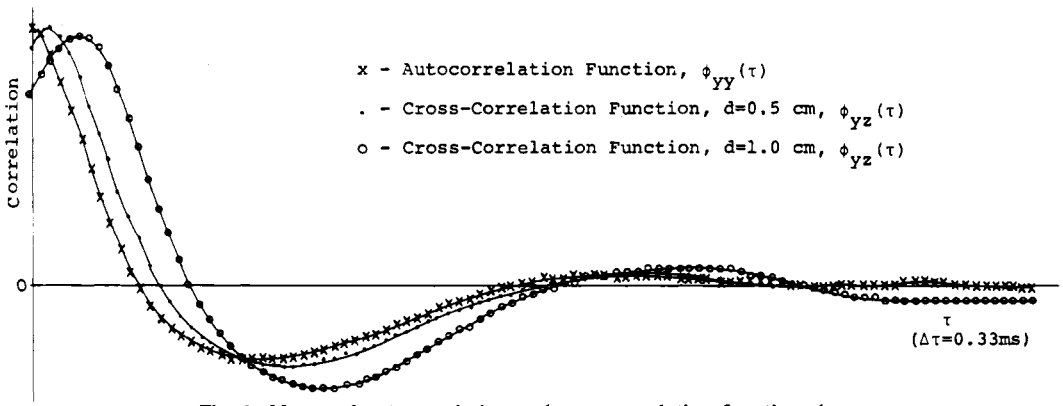

Fig. 6. Measured autocorrelation and cross-correlation functions (gross monopolar myoelectric signal).

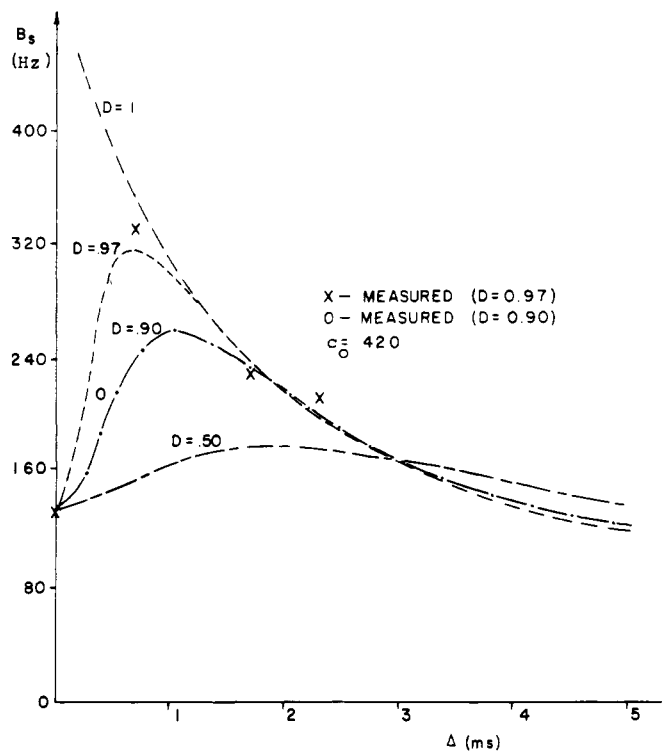

Fig. 7. Theoretical dependence of bipolar signal bandwidth on delay, with experimental data.

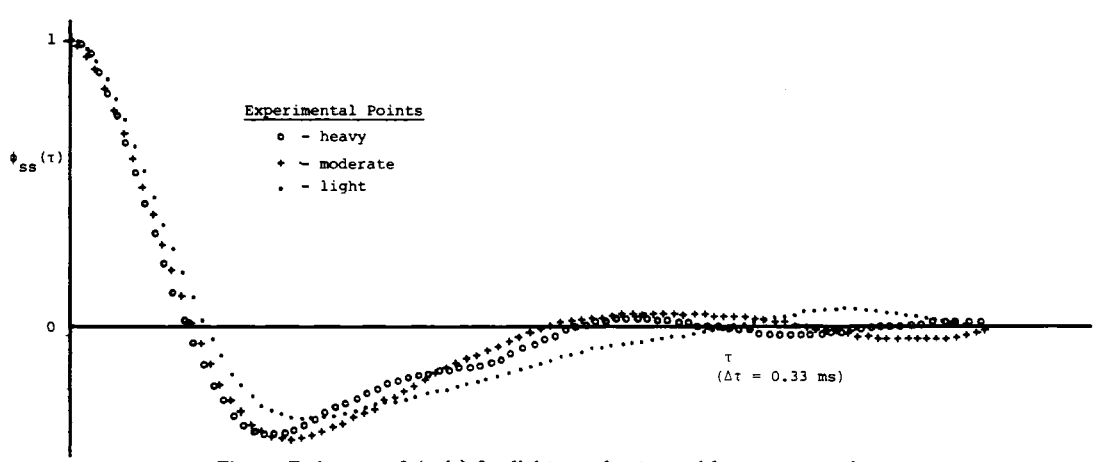

Fig. 8. Estimates of $\phi_{ss}(\tau)$ for light, moderate, and heavy contractions (curves normalized to peak values).

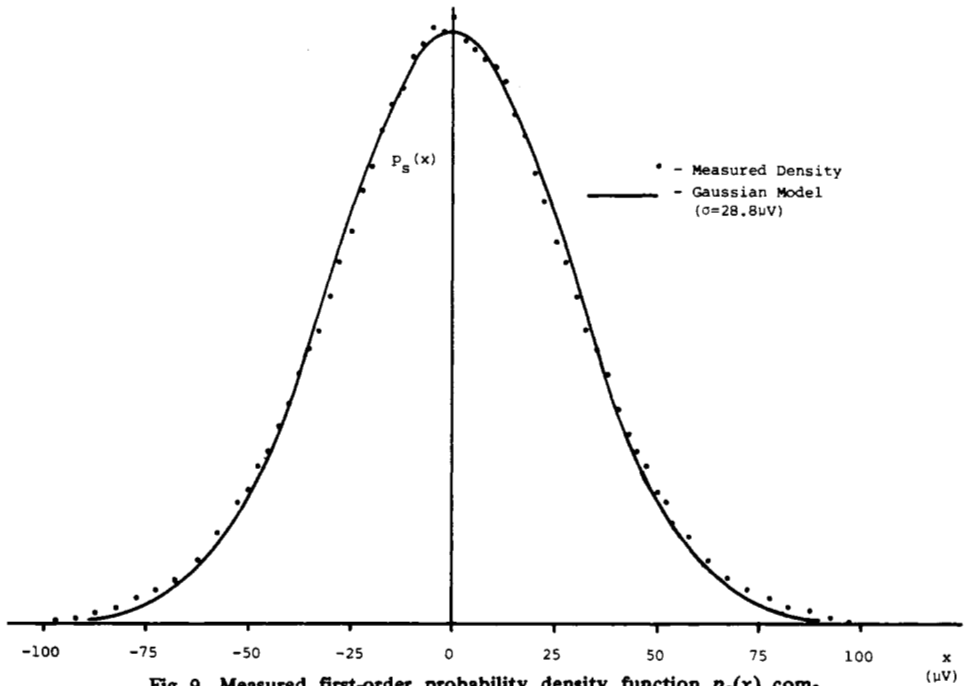

Fig. 9. Measured first-order probability density function $p_s(x)$ compared with Gaussian density (bipolar signal, moderate contractions).

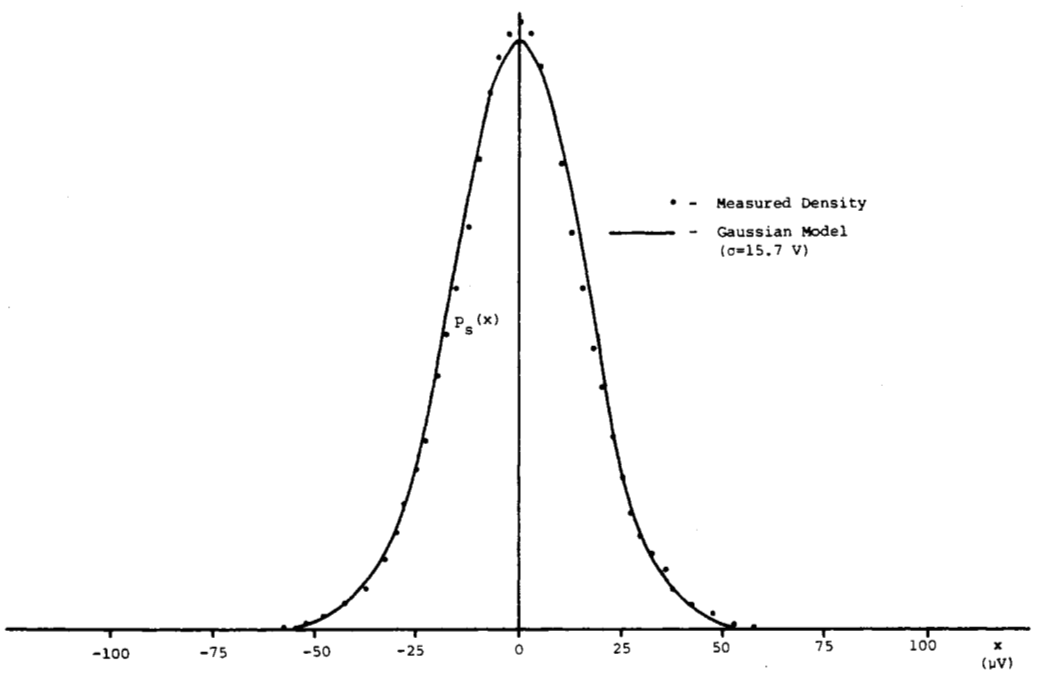

Fig. 10. Measured first-order probability density function $p_s(x)$ compared with Gaussian density (bipolar signal, light contraction).

are consistent with the spacings commonly used with electrodes in myoelectric systems. In order to avoid electrode movement light isometric contractions were used, and the first contraction was used as the data. Fig. 7 shows measured and theoretical values of B_s versus Δ, with the theoretical values obtained from (21). Fig. 8 shows estimates of $\phi_{ss}(\tau)$ for three levels of muscle contraction indicating that the form of $\phi_{ss}(\tau)$ is nearly independent of contraction level as predicted by (18). A heavy contraction was approximately 50 percent of the subject's maximum contraction, a moderate approximately 25 percent and the light just perceptable to the subject.

The probability density functions for the random process $s(t)$ depend on the statistics of the point processes $Q_j(t)$, $j = 1, 2, \cdots, N_a$, and on $p(t)$. As shown by Wozencraft and Jacobs [14] as $\lambda_p \to \infty$ $s(t)$ approaches a Gaussian process, and for λ_p^{-1} small compared to the time constant of $p(t)$, $s(t)$ will closely approximate a Gaussian process. In practice the range on λ_p is such that the Gaussian approximation is reasonably good. Figs. 9 and 10 show two measured first order probability density functions $p_s(x)$, for $s(t)$ at two levels of muscle con-

traction, along with Gaussian functions with the same variances. Similar results for the first-order density were found by Dhareshwar [15].

In summary the main points of this model are as follows:

1) The pooled motor unit firing rate λ_p alone reflects the contraction level and is thus the information parameter in the myoelectric signal.
2) The signal power is directly proportional to λ_p.
3) The form of the bipolar signal autocovariance function $\phi_{ss}(\tau)$ is independent of the contraction level (18).
4) The bipolar signal statistics can be written in terms of the monopolar signal statistics and the delay Δ which is proportional to the electrode spacing d.
5) The bipolar signal bandwidth depends on Δ for which there exists a value that maximizes B_s.
6) $s(t)$ is reasonably modelled as a Gaussian random process for values of λ_p of practical interest.

IV. Minimum Probability of Error Receiver

In this section, we seek the solution to the second of the two problems posed earlier, i.e., the determination of the optimum signal processing strategy. Since the first task of the myoelectric channel is to choose the correct prosthesis function, minimum probability of error is an obvious optimization criterion. The relevant myoelectric signal parameter is, from the model of Section III, the mean firing rate λ_p. The optimum set of parameter values is found in Section V.

For the multistate myoelectric channel the signal process under hypothesis H_i, $i = 0, 1, \cdots, M-1$, is a zero-mean stochastic process with autocovariance functions $\phi^i_{ss}(\tau)$ and with sample functions $s(t, \gamma_i)$. On all hypotheses there is present an additive white zero-mean Gaussian noise process $w(t)$ with spectral density $N_o/2$. Thus under hypothesis H_i the received signal $r(t)$ in the observation interval $[0, T]$ is

$$H_i: r(t) = s(t, \gamma_i) + w(t), \qquad [0, T], \quad i = 0, 1, \cdots, M-1.$$

The receiver must test the alternate hypotheses and accept one with the minimum probability of error. From (18) we have

$$\gamma_i = \lambda_{pi} \qquad \phi^i_{ss}(\tau) = \lambda_{pi} C(\tau) \tag{22}$$

where $C(\tau) = (\psi_a + \psi_b)\phi(\tau) - \psi_{ab}(\phi(\tau + \Delta) - \phi(\tau - \Delta))$ which is independent, for a given electrode configuration, of the hypotheses H_i, $i = 0, 1, \cdots, M-1$.

It is of interest to first consider the detection problem assuming access to the Poisson point process $\theta(t)$, of Fig. 3, which generates $s(t)$. This lends insight into the work to follow. From the likelihood ratio test it is straightforward to show that the number m of impulses of $\theta(t)$ in the interval $[0, T]$ is a sufficient statistic for the decision process [16]. In practice one does not have access to $\theta(t)$ and the detection problem must be formulated in terms of $s(t)$. However, since $s(t)$ is derived from $\theta(t)$, m will also be a sufficient statistic for that formulation.

Now formulating the M-ary detection problem in terms of $s(t, \gamma_i)$ and $w(t)$ we have

$$H_i: r(t) = s(t, \lambda_{pi}) + w(t), \qquad [0, T], \quad i = 0, 1, \cdots, M-1$$

where

$$s(t, \lambda_{pi}) = \sum_{j=1}^{m} \{a_j p(t - t_j) - b_j p(t - t_j - \Delta)\}$$

and again m is the number of impulses of $\theta(t)$ in $[0, T]$ or the number of action potential pulses in $[0, T]$. From above it is known that m is a sufficient statistic, and hence a solution to the problem is to attempt to estimate m by counting pulses in $r(t)$. The problem then becomes one of superresolving overlapping pulses in white Gaussian noise. Optimum solutions to this problem generally lead to complex receivers and disappointing performance [17], [18] even for small m and few pulse overlaps. For the case at hand m can range from a few hundred to several thousands, and there are a large number of pulse overlaps. Moreover, although an average pulse shape was used for the signal model, the action potential pulse shapes encountered in practice differ. In our view these facts strongly suggest the infeasibility of the "superresolution" approach to the practical solution of the myoelectric detection problem. However, the fact that m is large leads one to the possibility of approximating $s(t, \lambda_{pi})$ as a Gaussian process. Indeed as noted in Section III, $s(t)$ can be approximated as a Gaussian process for values of λ_p of practical interest in this paper.

With the Gaussian assumption the signal process $s(t, \gamma_i)$ becomes a zero-mean Gaussian process with variance σ_i^2, where from (22)

$$\sigma_i^2 = \lambda_{pi} C(0) \tag{23}$$

$$\phi^i_{ss}(\tau) = \sigma_i^2 C(\tau)/C(0) \tag{24}$$

and the detection problem becomes

$$H_i: r(t) = s(t, \sigma_i^2) + w(t), \qquad [0, T], \quad i = 0, 1, \cdots, M-1.$$

To proceed to the minimum probability of error receiver we obtain a vector representation $\bar{R}$, for $r(t)$ and set up the $M-1$ likelihood ratios $\Lambda_k[\bar{R}]$ $k = 1, 2, \cdots, M-1$. The likelihood ratios and the likelihood ratio tests are given by

$$\Lambda_k[\bar{R}] = \frac{p(\bar{R}|H_k)}{p(\bar{R}|H_0)} \underset{H_k^c}{\overset{H_0^c}{\gtrless}} \frac{P_0}{P_k}, \qquad k = 1, 2, \cdots, M-1.$$

where $p(\bar{R}|H_k)$ is the conditional probability density function for $\bar{R}$ given H_k, P_k is the *a priori* probability of the hypothesis H_k and the notation H_k^c denotes the complement of H_k. The details of the receiver solution are found in Appendix II. There it is shown that T the receiver takes the form given in Fig. 11 where the quantities l_k are given by

$$l_k = N_o^{-1} \int_0^T dz \left[\int_0^T r(t)\, h_{fk}(z - t)\, dt \right]^2, \qquad k = 1, 2, \cdots, M-1, \tag{25}$$

the filters $H_{fk}(j\omega)$ are given by

$$H_{fk}(j\omega) = |\Phi^k_{ss}(\omega)/(\Phi^k_{ss}(\omega) + N_o/2)|^{1/2}, \qquad k = 1, 2, \cdots, M-1, \tag{26}$$

and the decision boundaries η_k are for equally likely hypotheses given by

$$\eta_k = -(T/4\pi) \int_{-\infty}^{\infty} \ln [1 + 2\Phi^k_{ss}(\omega)/N_o]\, d\omega, \qquad k = 1, 2, \cdots, M-1 \tag{27}$$

where $\Phi^k_{ss}(\omega)$ is the Fourier transform of $\phi^k_{ss}(\tau)$.

It is seen from Fig. 11 that the receiver requires $M-1$ parallel processors and has an $M-1$ dimensional decision space. This complexity is clearly undesirable in a practical multistate myoelectric system.

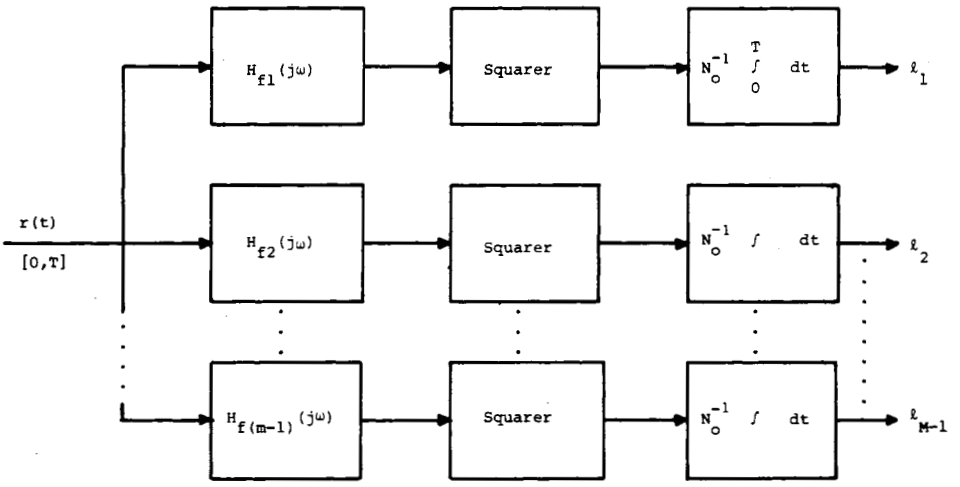

Fig. 11. Bayes receiver for Gaussian myoelectric signal in white Gaussian noise (stationary processes and long observation interval).

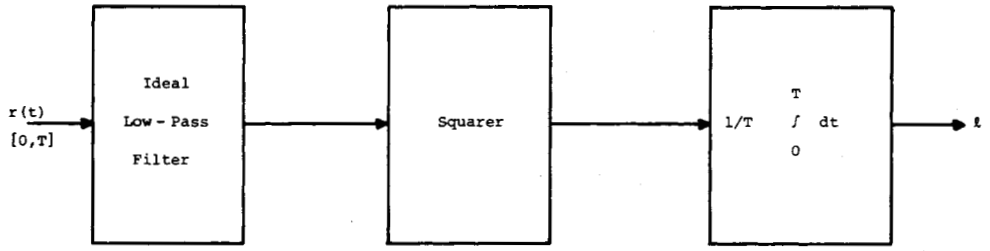

Fig. 12. Bayes receiver for bandlimited white Gaussian signal process in white Gaussian noise.

The signal to noise power ratios in most cases are such that all the $H_{fk}(j\omega)$, $k = 1, 2, \cdots, M-1$, are reasonably well approximated by ideal low-pass filters with bandwidths ω_o and gains $\sigma_k^2/(\sigma_k^2 + \sigma_o^2)$ where σ_o^2 is the noise power in bandwidth $2\omega_o$. In this case each filter gain can be incorporated with its associated η_k, $k = 1, 2, \cdots, M-1$, on the decision boundary side of the log likelihood ratio test. This leaves all filters identical and hence a single common filter suffices. The quantities l_k, $k = 1, 2, \cdots, M-1$, are thus identical and independent of k and the receiver has a one-dimensional decision space. This approximation is equivalent to approximating $s(t, \sigma_i^2)$ as a bandlimited white Gaussian process with

$$\Phi_{ss}^k(\omega) = \begin{cases} \sigma_k^2/2\omega_o, & -\omega_o \leqslant \omega \leqslant \omega_o \\ 0, & \text{otherwise.} \end{cases} \tag{28}$$

That this is a reasonable first-order approximation is shown by Parker [19]. With the approximation of (28) the receiver and decision regions follow immediately from (25)–(27). Equation (26) gives the ideal low-pass filters with bandwidths ω_o and gains $\sigma_k^2/(\sigma_k^2 + \sigma_o^2)$ as discussed above. Equation (27) gives

$$\eta_k = (-T\omega_o/2\pi) \ln (1 + \sigma_k^2/\sigma_o^2) \tag{29}$$

Denoting the common statistic as l and the common low-pass filter as $h_f(v - t)$, the log likelihood ratio test becomes from (25) and (29),

$$l = \left(\frac{1}{T}\right)\int_0^T \left[\int_0^T r(t)\, h_f(v-t)\, dt\right]^2 dv \underset{H_k^c}{\overset{H_i^c}{\gtrless}} \left[\frac{\sigma_{kT}^2\sigma_{iT}^2}{(\sigma_{kT}^2 - \sigma_{iT}^2)}\right] \cdot \ln\left(\frac{\sigma_{kT}^2}{\sigma_{iT}^2}\right), \quad k = 1, 2, \cdots, M-1 \text{ and } i = k-1. \tag{30}$$

where $\sigma_{kT}^2 = \sigma_k^2 + \sigma_o^2$, H_k^c denotes the complement of H_c and $\sigma_1^2 < \sigma_2^2 < \cdots < \sigma_{M-1}^2$. This receiver is shown in Fig. 12 and the decision boundaries are such that it chooses

$$H_0 \text{ if } l < [\sigma_{1T}^2\sigma_o^2/(\sigma_{1T}^2 - \sigma_o^2)] \ln \sigma_{1T}^2/\sigma_o^2 \tag{31}$$

$$H_{M-1} \text{ if } l > [\sigma_{(M-1)T}^2\sigma_{(M-2)T}^2/(\sigma_{(M-1)T}^2 - \sigma_{(M-2)T}^2)] \cdot \ln (\sigma_{(M-1)T}^2/\sigma_{(M-2)T}^2) \tag{32}$$

and

$$H_i, \quad i = 1, 2, \cdots, M-2, \text{ if } [\sigma_{iT}^2\sigma_{(i-1)T}^2/(\sigma_{iT}^2 - \sigma_{(i-1)T}^2)] \cdot \ln (\sigma_{iT}^2/\sigma_{(i-1)T}^2) \leqslant l \leqslant [\sigma_{iT}^2\sigma_{(i+1)T}^2/(\sigma_{(i+1)T}^2 - \sigma_{iT}^2)] \cdot \ln (\sigma_{(i+1)T}^2/\sigma_{iT}^2). \tag{33}$$

V. Optimum Signal Set

The optimum receiver decision regions of Section IV were found for an arbitrary set, $\{\sigma_{iT}^2\}$ of variances. Given the noise variance σ_o^2 and the maximum myoelectric signal variance σ_m^2, we now ask what is the optimum set σ_{iT}^2, $i = 0, 1, \cdots, M-1$, to achieve minimum probability of error?

Consider the expression for the probability of error $P(E)$

$$P(E) = 1 - M^{-1}\sum_{i=0}^{M-1}\int_{z_i} p(l|H_i)\, dl \tag{34}$$

where $p(l|H_i)$ is the probability density function for l given H_i and Z_i is the decision space region over which the hypothesis H_i is true. Equations (31)–(33) define z_i, $i = 0, 1, \cdots, M-1$. With σ_o^2 and $\sigma_{(M-1)T}^2$ given, the optimum set is found by minimizing (34) over σ_{iT}^2, $i = 1, \cdots, M-2$. Since l is the result of a squaring and integrating operation $p(l|H_i)$ can be closely approximated by a chi-square function [19]. A numerical minimization of (34) was carried out by digital computer. Two sig-

TABLE I
RECEIVER MEASURED PERFORMANCE (STATIC) COMPARED WITH THE THEORETICAL PERFORMANCE (SUBJECTS E. D. AND M. K.)

M	T (s)	P(E) (measured) E.D.	M.K.	P(E) (theoretical)	Expected Standard Deviation
2	0.05	0.0	0.0	0.000	-
4	0.05	0.011	0.011	0.007	0.003
6	0.05	0.111	0.138	0.092	0.010
8	0.05	0.247	0.258	0.219	0.015
10	0.05	0.352	0.379	0.332	0.018
2	0.15	0.0	0.0	0.000	-
4	0.15	0.0	0.0	0.000	-
6	0.15	0.010	0.008	0.006	0.002
8	0.15	0.060	0.044	0.043	0.007
10	0.15	0.129	0.119	0.113	0.011

TABLE II
RECEIVER MEASURED PERFORMANCE (STATIC) COMPARED WITH THE THEORETICAL PERFORMANCE (INTEGRATOR REPLACED BY A FIRST-ORDER LOW-PASS FILTER, SUBJECTS T. R. AND R. C.)

M	T (s)	P(E) (measured) T.R.	R.C.	P(E) (theoretical)	Expected Standard Deviation
2	0.05	0.0	0.0	0.000	-
4	0.05	0.060	0.082	0.054	0.007
6	0.05	0.249	0.278	0.224	0.015
8	0.05	0.369	0.374	0.373	0.019
10	0.05	0.494	0.536	0.482	0.023
2	0.15	0.0	0.0	0.000	-
4	0.15	0.005	0.009	0.003	0.002
6	0.15	0.085	0.090	0.061	0.008
8	0.15	0.200	0.220	0.173	0.013
10	0.15	0.320	0.347	0.283	0.017

nificant results were obtained. First the optimum values of σ_{iT}^2 were found to increase exponentially with i from σ_o^2. An empirical expression which gives this result is

$$\sigma_{iT}^2 = \sigma_o^2 \exp\left[(i/M - 1)\ln(1 + \sigma_m^2/\sigma_o^2)\right], \quad i = 0, 1, \cdots, M-1. \quad (35)$$

Secondly the optimum signal set is independent of the observation interval length T.

VI. Receiver Performance

The theoretical performance $P(E)$ of the receiver of Section IV with its optimum signal set is obtained by evaluating (34) with $p(l|H_i)$ taken to be a chi-square function. The mean and variance of l given H_i are easily shown to be σ_{iT}^2 and σ_{iT}^2/B_sT, respectively, where B_s is the equivalent statistical bandwidth of the squarer input signal. The optimum values of σ_{iT}^2 were obtained from (35) and the z_i subsequently found from (31)-(33). Equation (34) was then evaluated numerically for various values of M and T and the results given in Table I. The theoretical performance was also computed for the case of a first order low-pass filter, with a time constant of $T/5$, replacing the integrator of Fig. 12. These results are given in Table II.

A series of experiments was carried out to verify the computed performance results. In order to obtain data relatively free of operator error and hence reflect the receiver performance only, the experiment is static. It is static in that the operator is asked to maintain, with the aid of visual feedback, a given signal level σ_{iT}^2 for a period of time T_r. This period is broken up into blocks of duration T seconds and for each block the receiver processes the signal and makes a decision as to the correct hypothesis. Hence a sequence of $N_r = T_r/T$ decisions is obtained from which an estimate, $\hat{P}(E|H_i)$, of $P(E|H_i)$ is found by taking the ratio of the number of errors, n_e, to N_r, i.e.,

$$\hat{P}(E|H_i) = n_e/N_r.$$

This is repeated for all σ_{iT}^2, $i = 0, 1, \cdots, M-1$, and an estimate $\hat{P}(E)$ of $P(E)$ obtained from

$$\hat{P}(E) = M^{-1} \sum_{i=0}^{M-1} \hat{P}(E|H_i).$$

TABLE III
THEORETICAL PERFORMANCE FIGURES FOR THE CONVENTIONAL RECEIVER $P_1(E)$, THE BAYES RECEIVER $P_2(E)$ AND THE BAYES RECEIVER WITH THE INTEGRATOR REPLACED BY A LOW-PASS FILTER $P_3(E)$

M	T (s)	$P_1(E)$	$P_2(E)$	$P_3(E)$
2	0.05	0.028	0.000	0.000
4	0.05	0.215	0.007	0.054
6	0.05	0.377	0.092	0.224
8	0.05	0.484	0.219	0.373
10	0.05	0.560	0.332	0.482
2	0.15	0.003	0.000	0.000
4	0.15	0.104	0.000	0.003
6	0.15	0.244	0.006	0.061
8	0.15	0.353	0.043	0.173
10	0.15	0.435	0.113	0.283

The results are given in Table I and Table II along with the calculated performance figures. The agreement is seen to be reasonably good. Also given in Tables I and II is the "Expected Standard Deviation" for the measured values of $P(E)$. This is the measured data standard deviation which can be expected based on the theoretical values of $P(E)$, and is shown [19] to be approximately given by

$$\text{Expected Standard Deviation} \simeq (P(E)/N_r)^{1/2}.$$

Table III compares the theoretical performance of the Bayes receiver with the theoretical performance of a receiver which is

somewhat typical of receivers now used in the myoelectric channel. This receiver is a full-wave rectifier and low-pass filter with a time constant of $T/5$ seconds. The signal parameter set consists of signal mean absolute values equally spaced over the signal range, and the decision boundaries are placed midway between successive mean absolute values. A significant improvement is seen with the Bayes minimum probability of error receiver.

VII. Results

The principal results of this paper are now summarized. First a practically useful model for the bipolar myoelectric signal was developed. This model clearly implies that the relevant signal parameter in the myoelectric channel is the mean firing rate λ_p. The model also implies that the signal autocovariance function form is independent of muscle contraction level and this was shown to be experimentally valid. This fact was significant to the work on the optimum receiver. Second the minimum probability of error receiver, for a stationary Gaussian signal process and long observation interval, was found for the myoelectric channel. With some simplification a form was obtained for this receiver which requires the computation of one statistic only and hence has a one-dimensional decision space—a desirable characteristic for practical implementation. Third the optimum signal set $\{\sigma_i^2,\ i = 0, 1, \cdots, M-1\}$, was found for the minimum probability of error receiver. The measured performance figures agree well with the theoretical performance figures for the optimum receiver. The optimum receiver shows a marked performance improvement over the more conventional receiver.

VIII. Discussion

The significance of the work described in this paper is that it gives the information required to approach the optimum myoelectric channel for the patient. That is, with the optimum receiver, the patient is given the potential of achieving the lowest error probability possible in the selection of the prosthesis functions. This of course holds only for the single-muscle myoelectric control system—referred to here as the multistate system. It is important to note that the error rates possible with this system will only be achieved if the patient can learn to generate the appropriate signal levels. The receiver cannot recognize a situation in which the patient generates a signal level different from that intended. It should be noted that the receiver derived holds for all values of M.

The receiver is not difficult to realize nor does it differ greatly from those in use. The marked improvement in performance is obtained from the solution to the detection problem which gives the optimum decision boundaries and the optimum signal set. One can view the effect of the improved performance in two ways. First a given error probability, for a given task, should be more easily achieved, i.e., with less patient training. Second, performance improvement with training should be more marked since the minimum error bound is considerably lower than for the more typical receiver.

The optimum receiver with its well defined decision boundaries, and the optimum signal set make it possible to "set" the system for a given patient. Given the system noise level and the measured useable myoelectric signal range the signal set and decision boundaries are easily calculated. These can be set and left, with adjustments required only if the patient's signal range changes.

It is interesting to note that with the optimum receiver there is little point in using a filter time constant in excess of approximately 30 ms for $M \leqslant 4$. From Table II it is seen that for $M = 4$ and a time constant of 30 ms the receiver error is approximately 0.003. At this small value the operator error will almost certainly dominate, and increasing the filter time constant will not significantly alter the system error. As the operator error decreases with training to become comparable to 0.003, then increasing the time constant may be advantageous.

Some of the results of this research are currently being used in a three-state myoelectric system for the control of powered upper limb prostheses at the University of New Brunswick, Fredericton, N.B., Canada.

Appendix I
Correlation Functions $R_{QQ}(\tau)$, $R_{PP}(\tau)$, and $R_{QP}(\tau)$

Given the stationary Poisson point process $Q(t)$, where

$$Q(t) = \sum_{k=1}^{\infty} a_k \delta(t - t_k)$$

with mean firing rate λ_p and impulse intensities a_k, it is desired to find the autocorrelation function $R_{QQ}(t_1, t_2)$ of the process $Q(t)$. The a_k are independent random variables with

$$E[a_k] = \mu_a \quad \text{and} \quad E[a_k^2] = \psi_a.$$

An approach is used which is similar to that used by Papoulis to find the autocorrelation function of a Poisson point process with constant impulse intensities [20].

Consider the process $s(t)$ such that $s(0) = 0$ and

$$s(t_1) = \sum_{i=1}^{n_1} a_i$$

where n_1 is the number of impulses of the Poisson point process $Q(t)$ in the interval $[0, t_1]$ and the a_i are the impulse intensities.

The autocorrelation function $R_{ss}(t_1, t_2)$ of $s(t)$ is

$$\begin{aligned} R_{ss}(t_1 t_2) &= E[s(t_1)s(t_2)] \\ &= E\left[\sum_{i=1}^{n_1} a_i \sum_{j=1}^{n_2} a_j\right] \\ &= E\left[\sum_{i=1}^{n_1}\sum_{j=1}^{n_2} a_i a_j\right] \end{aligned} \tag{A1.1}$$

where n_2 is the number of impulses in the interval $[0, t_2]$. Now using the identity

$$E[s(t_1)s(t_2)] = E\{E[s(t_1)s(t_2)|n_1, n_2]\}$$

and letting $t_2 > t_1$, equation (A1.1) becomes

$$R_{ss}(t_1, t_2|n_1, n_2) = \sum_{i=1}^{n_1}\sum_{j=1}^{n_2} E[a_i a_j|n_1, n_2], \qquad t_2 > t_1$$

and since the $a_i a_j$ are independent of n_1 and n_2 this becomes

$$\begin{aligned} R_{ss}(t_1, t_2|n_1, n_2) &= \sum_{i=1}^{n_1}\sum_{j=1}^{n_2} E[a_i a_j], && t_2 > t_1 \\ &= n_1 E[a_i^2] + (n_1 n_2 - n_1)E[a_i a_j], && t_2 > t_1 \end{aligned}$$

and with the a_i independent of the a_j,

$$R_{ss}(t_1, t_2|n_1, n_2) = n_1 \psi_a + \mu_a^2(n_1 n_2 - n_1), \qquad t_2 > t_1$$

Now let $n_2 - n_1 = \epsilon$ where ϵ is the number of impulses in the

interval $[t_2, t_1]$ and hence

$$R_{ss}(t_1, t_2 | n_1, n_2) = n_1 \psi_a + \mu_a^2(n_1^2 + n_1 \epsilon - n_1) \qquad t_2 > t_1 \tag{A1.2}$$

and with $R_{ss}(t_1, t_2) = E[R_{ss}(t_1 t_2 | n_1, n_2)]$, equation (A1.2) gives

$$R_{ss}(t_1, t_2) = \psi_a E[n_1] + \mu_a^2\{E[n_1^2] + E[n_1 \epsilon] - E[n_1]\}, \qquad t_2 > t_1$$

and since n_1 and ϵ are independent

$$\begin{aligned} R_{ss}(t_1, t_2) &= \psi_a E[n_1] + \mu_a^2\{E[n_1^2] + E[n_1]\,E[\epsilon] - E[n_1]\}, \qquad t_2 > t_1 \\ &= \psi_a \lambda_p t_1 + \mu_a^2\{\lambda_p^2 t_1^2 + \lambda_p t_1 + \lambda_p^2 t_1(t_2 - t_1) \\ &\quad - \lambda_p t_1\}, \qquad t_2 > t_1 \\ &= \psi_a \lambda_p t_1 + \mu_a^2 \lambda_p^2 t_1 t_2, \qquad t_2 > t_1 \end{aligned} \tag{A1.3}$$

Similarly for $t_1 > t_2$

$$R_{ss}(t_1, t_2) = \psi_a \lambda_p t_2 + \mu_a^2 \lambda_p^2 t_1 t_2, \qquad t_1 > t_2 \tag{A1.4}$$

and for $t_1 = t_2$ it is easily seen that $R_{ss}(t_1, t_2)$ is given by either (A1.3) or (A1.4).

For all values of t, $R_{ss}(t_1, t_2)$ can be written as

$$\begin{aligned} R_{ss}(t_1, t_2) &= [\psi_a \lambda_p t_2 + \mu_a^2 \lambda_p^2 t_1 t_2]\, u(t_1 - t_2) \\ &\quad + [\psi_a \lambda_p t_1 + \mu_a^2 \lambda_p^2 t_1 t_2](1 - u(t_1 - t_2)) \end{aligned} \tag{A1.5}$$

where $u(t)$ is the unit step function.

The Poisson point process $Q(t)$ can be generated by taking the derivative of $s(t)$ with respect to t, i.e.,

$$Q(t) = \frac{ds(t)}{dt}$$

and hence

$$R_{QQ}(t_1, t_2) = \frac{\partial^2 R_{ss}(t_1, t_2)}{\partial t_1 \partial t_2}. \tag{A1.6}$$

Carrying out the indicated operations in (A1.6) gives

$$R_{QQ}(t_1, t_2) = \psi_a \lambda_p \delta(t_1 - t_2) + \mu_a^2 \lambda_p^2$$

and letting $t_1 - t_2 = \tau$ this becomes

$$R_{QQ}(\tau) = \psi_a \lambda_p \delta(\tau) + \mu_a^2 \lambda_p^2.$$

Similarly it can be shown that

$$R_{PP}(\tau) = \psi_b \lambda_p \delta(\tau) + \mu_b^2 \lambda_p^2$$

and

$$R_{QP}(\tau) = \psi_{ab} \lambda_p \delta(\tau - \Delta) + \mu_a \mu_b \lambda_p^2$$

where

$$E[b_k] = \mu_b, E[b_k^2] = \psi_b$$

and

$$\begin{aligned} E[a_i b_j] &= \psi_{ab}, \qquad \text{for } i = j \\ &= \mu_a \mu_b, \qquad \text{for } i \neq j. \end{aligned}$$

Appendix II
Minimum Probability of Error Receiver

The Karhunen–Loève expansion of $r(t)$ is obtained using the eigenfunctions $\omega_j(t)$, $j = 1, \cdots, \infty$, of $s(t, \sigma_i^2)$ as the complete orthonormal set where $\omega_j(t)$ and its eigenvalue λ_j are found from the solution of

$$\lambda_j \omega_j(t) = \int_0^T \phi_{ss}^i(t, u)\, \omega_j(u)\, du, \qquad 0 \leqslant t \leqslant T.$$

It is important to note that as a result of (24) the eigenfunctions are identical under all hypotheses and the eigenvalues differ by the scale factor σ_i^2. An L term approximation to $r(t)$ is constructed from

$$r_L(t) = \sum_{j=1}^{L} r_j \omega_j(t)$$

where

$$r_j = \int_0^T [s(t, \sigma_i^2) + w(t)]\, \omega_j(t)\, dt,$$

$$E[r_j | H_i] = 0$$

$$E[r_j^2 | H_i] = \sigma_i^2 \lambda_j + N_o/2.$$

Due to the Karhunen–Loève expansion and the Gaussian assumption, the r_j, $j = 1, \cdots, \infty$, are independent Gaussian random variables under all hypotheses. Thus with $\overline{R} = (r_1, \cdots, r_L)$ and with $p(\overline{R}|H_k)$ the conditional probability density function for $\overline{R}$ given H_k, the log likelihood ratios are

$$\begin{aligned} \ln \Lambda_k[r_L(t)] &= \ln [p(\overline{R}|H_k)/p(\overline{R}|H_0)], \qquad k = 1, 2, \cdots, M - 1 \\ &= N_o^{-1} \sum_{j=1}^{L} \sigma_k^2 \lambda_j r_j^2 / (\sigma_k^2 \lambda_j + N_o/2) \\ &\quad - 2^{-1} \sum_{j=1}^{L} \ln (1 + 2\sigma_k^2 \lambda_j / N_o). \end{aligned} \tag{A2.1}$$

The closed form for (A2.1) as $L \to \infty$ is obtained by Van Trees [21] as

$$\ln \Lambda_k[r(t)] = N_o^{-1} \int_0^T \int_0^T r(t)\, h_k(t, v)\, r(v)\, dt\, dv - \eta_k \tag{A2.2}$$

where $h_k(t, v)$ is the solution to

$$N_o h_k(t, v)/2 + \int_0^T h_k(t, z)\, \phi_{ss}^k(z, v)\, dz = \phi_{ss}^k(t, v), \qquad 0 \leqslant t, v \leqslant T \tag{A2.3}$$

and

$$\eta_k = 2^{-1} \sum_{j=1}^{\infty} \ln (1 + 2\sigma_k^2 \lambda_j / N_0) \tag{A2.4}$$

The filter-squarer-integrator realization of this receiver due to Van Trees [21] is

$$\ln \Lambda_k[r(t)] = l_k = N_o^{-1} \int_0^T dz \left[\int_0^T r(t)\, h_{fk}(z, t)\, dt \right]^2 \tag{A2.5}$$

where $h_{fk}(t, z)$ is the solution of

$$h_k(t, v) = \int_0^T h_{fk}(z, v)\, h_{fk}(z, t)\, dz, \qquad 0 \leqslant t, \quad v \leqslant T. \tag{A2.6}$$

For all cases of interest here the observation interval is long compared to the time required for system transients to decay and the processes are stationary. Hence asymptotic solutions as $T \to \infty$ are acceptable [21]. The asymptotic solutions to (A2.3), (A2.4), and (A2.6) give

$$H_{fk}(j\omega) = |\Phi_{ss}^k(\omega)/(\Phi_{ss}^k(\omega) + N_o/2)|^{1/2}, \qquad k = 1, \cdots, M-1 \tag{A2.7}$$

and

$$\eta_k = -(T/4\pi) \int_{-\infty}^{\infty} \ln\,[1 + 2\Phi_{ss}^k(\omega)/N_o]\, d\omega, \qquad k = 1, \cdots, M-1 \tag{A2.8}$$

where $\Phi_{ss}^k(\omega)$ is the Fourier transform of $\phi_{ss}^k(\tau)$.

References

[1] D. S. Dorcas, V. A. Dunfield, and R. N. Scott, "Improved myoelectric control system," *Medical and Biological Eng.*, vol. 8, no. 4, pp. 333-341, July 1970.

[2] R. N. Scott, P. A. Parker, and V. A. Dunfield, "Myoelectric control," in *IEE Medical Electronics Monographs* 7-12, B. W. Watson and D. W. Hill, Eds. London, England: Peter Perigrinus Ltd., pp. 141-169.

[3] J. G. Kreifeldt, "Signal versus noise characteristics of filtered EMG used as a control source," *IEEE Trans. Bio-Med. Eng.*, vol. BME-18, pp. 16-22, Jan. 1971.

[4] D. Graupe, W. K. Cline, and T. K. Kaplon, "Stochastic analysis of EMG signals for multi-functional prosthesis control purposes," in *Proc. 1973 Carnahan Conf. on Electronic Prosthetics*, Lexington, KY, 1973.

[5] L. A. Geddes, *Electrodes and the Measurement of Bioelectric Events*. New York: Wiley-Interscience, 1972, pp. 251-257.

[6] G. Brody, R. N. Scott, and R. Balasubramanian, "A model for myo-electric signal generation," *Medical and Biological Eng.*, vol. 12, no. 1, pp. 29-41, Jan. 1974.

[7] H. P. Clamman, "A quantitative analysis of the firing patterns of single motor units of a skeletal muscle of man and their utilization in isometric contractions," Ph.D. dissertation, John Hopkins Univ., Baltimore, MD, 1967.

[8] E. Shwedyk, "Estimation of a muscle's force from its myo-electric signal during nonisometric contractions," Ph.D. dissertation, Univ. New Brunswick, Fredericton, N.B., Canada, 1973.

[9] P. A. Parker and R. N. Scott, "Statistics of the myoelectric signal from monopolar and bipolar electrodes," *Medical and Biological Eng.*, vol. 11, no. 5, pp. 591-596, Sept. 1973.

[10] D. R. Cox and N. L. Smith, "On the superposition of renewal processes," *Biometrica*, vol. 41, pp. 91-99, 1954.

[11] A. Papoulis, *Probability, Random Variables, and Stochastic Processes*. New York: McGraw-Hill, 1965, pp. 345-352.

[12] J. S. Bendat and A. G. Piersol, *Measurement and Analysis of Random Data*. New York: Wiley, 1966, p. 265.

[13] F. Buchtal, C. Guld, and P. Rosenfalck, "Innervation zone and propagation velocity in human muscle," *Acta Physiologica Scandinavica*, vol. 35, pp. 174-190, 1956.

[14] J. M. Wozencraft and I. M. Jacobs, *Principles of Communication Engineering*. New York: Wiley, 1965, pp. 144-179.

[15] L. Dhareshwar, "Crosstalk in myo-electric control systems," M.Sc. thesis, Univ. New Brunswick, Fredericton, N.B., Canada, 1967.

[16] H. L. Van Trees, *Detection, Estimation, and Modulation Theory, Part I*. New York: Wiley, 1968, p. 29.

[17] J. A. Stuller, "Generalized likelihood signal resolution," *IEEE Trans. Inform. Theory*, vol. IT-21, pp. 268-282, May 1975.

[18] N. J. Nilsson, "On the optimum range resolution of radar signals in noise," *IRE Trans. Inform. Theory*, vol. IT-7, pp. 245-253, Oct. 1961.

[19] P. A. Parker, "Optimum signal processing for a multistate myoelectric communication channel," Ph.D. dissertation, Univ. New Brunswick, Fredericton, N.B., Canada 1975.

[20] Papoulis, *op. cit.*, pp. 284-287.

[21] H. L. Van Trees, *Detection, Estimation and Modulation Theory, Part III*. New York: Wiley, 1971.

Pattern Recognition of Multiple EMG Signals Applied to the Description of Human Gait

GEORGE A. BEKEY, FELLOW, IEEE, CHI-WU CHANG, JACQUELINE PERRY, AND M. MARK HOFFER

Abstract—**The application of pattern recognition to the classification of normal and four pathological gaits is described. The classification is based on construction of a pattern feature vector whose elements are obtained by processing EMG signals obtained from 6 muscles responsible for movement of the foot at the ankle. The paper describes the basic actions of these muscles and the resulting gait patterns. Data were obtained from 30 patients at Rancho Los Amigos Hospital. 11 sets of data were used as training patterns for the synthesis of linear discriminant functions needed in the classification algorithm. The resulting algorithm was used to process 19 patient records. The correct gait was identified in 15 of these 19 sets. Potential clinical applications of the results are discussed.**

Manuscript received June 8, 1976; revised October 24, 1976. This work was supported in part by a Grant from the United Cerebral Palsy Research and Educational Foundation.

G. A. Bekey and C. W. Chang are with the Department of Electrical Engineering, University of Southern California, Los Angeles, CA 90007.

J. Perry and M. Hoffer are with the Rancho Los Amigos Hospital, Downey, CA.

I. Introduction

NORMAL HUMAN gait is accomplished by the coordinated activity of many muscles acting at the hip, knee, and ankle joints. Both the strength and timing of muscular contractions are controlled to accomplish the remarkable smoothness of forward movement during walking. If the pat-